Mon. Not. R. Astron. Soc. **340,** 289–303 (2003)

Extreme galactic wind and Wolf–Rayet features in infrared mergers and infrared quasi-stellar objects

S. Lípari,[1⋆†] R. Terlevich,[2‡] R. J. Díaz,[3†] Y. Taniguchi,[4] W. Zheng,[5†] Z. Tsvetanov,[5] G. Carranza[1] and H. Dottori[6]

[1]*Córdoba Observatory and CONICET, Laprida 854, 5000 Córdoba, Argentina*
[2]*Institute of Astronomy, Madingley Road, Cambridge CB3 0HA*
[3]*Córdoba Observatory and SeCyT, Universidad Nacional de Córdoba, Argentina*
[4]*Astronomical Institute, Tohoku University, Aoba, Sendai 980-8578, Japan*
[5]*Department of Physics & Astronomy, University of Johns Hopkins, Baltimore, MD 21218, USA*
[6]*Instituto de Física, Univ. Fed. Río Grande do Sul, CP 15051, Porto Alegre, Brazil*

Accepted 2002 November 22. Received 2002 September 17; in original form 2002 July 2

ABSTRACT

We report, as a part of a long-term study of infrared (IR) mergers and IR quasi-stellar objects (QSOs), detailed spectroscopic evidence for outflow (OF) and Wolf–Rayet (WR) features in the nearby mergers NGC 4038/39 and IRAS 23128−5919 (with low-velocity OF); and the nearby QSOs IRAS 01003−2238 and 13218+0552 (with extreme velocity OF, EVOF). We also study the presence of EVOF in a complete sample of ultraluminous IR galaxies and QSOs ('The IRAS 1-Jy Survey', 118 objects). We found EVOF in IRAS 11119+3257, 14394+5332, 15130−1958 and 15462−0450.

The low-velocity OF components were detected mainly in objects with starburst processes, i.e. OF associated with galactic winds generated in multiple type II supernova (SN) explosions and massive stars. Meanwhile the EVOF were detected mainly in objects with strong starburst plus obscured IR QSOs; which suggests that the coexistence of both processes could generate EVOF.

Hubble Space Telescope (*HST*) images of IR+BAL+Fe II QSOs show in practically all of these objects 'arc or shell' features probably associated with galactic winds [i.e. with multiple type II SN explosions or with starburst+active galactic nuclei (AGN)] or merger processes.

In addition, we analyse the presence of Wolf–Rayet features in part of the large sample of bright PG-QSOs. We found possible WR features in the Fe II PG-QSOs PG 1244+026, 1444+407, 1448+273 and 1535+547.

The results are discussed mainly within the framework of the composite scenario: starburst+AGN. We analyse the presence of extreme starburst and galactic winds as a possible link between IR mergers and IR QSOs. Finally, we discuss the probable role of mergers, extreme starburst and galactic winds processes in BAL-QSOs and galaxies in formation.

Key words: ISM: bubbles – galaxies: interactions – quasars: general – galaxies: starburst – infrared: galaxies.

1 INTRODUCTION

The main current issues in astrophysics are the study of mergers, extreme star formation processes, infrared (IR)/BAL quasi-stellar objects (QSOs) and the relations between them. These issues play an important role in practically every scenario of formation and evolution of galaxies and active galactic nuclei (AGNs) (for references see Sanders & Mirabel 1996 and Section 4.3). In addition, the presence of galactic winds (GWs) – associated mostly with extreme/massive star formation processes[1] – is also an important component for

⋆E-mail: lipari@mail.oac.uncor.edu
†Visiting astronomer at: ESO, BALEGRE, CASLEO Observatories.
‡Visiting scientist at: Instituto Nacional de Astrofísica, Óptica y Electrónica. AP 51, 72000 Puebla, Mexico.

[1] In this paper we use 'massive star formation process', as a large-scale phenomenon of vigorous massive star formation activity similar to 'starburst': regions with a strongly enhanced high-mass star formation rate.

different theoretical models of galaxy formation (see Ostriker & Cowie 1981; Berman & Suchkov 1991).

Mergers are mainly luminous IR galaxies for which the luminosities overlap with most luminous Seyfert galaxies and QSOs; and their optical, IR and radio properties show starburst and AGN characteristics (Joseph & Wright 1985; Schweizer 1980, 1982; Schweizer 1996; Rieke et al. 1985; Sanders et al. 1988a; Sanders & Mirabel 1996). Luminous IR galaxies ($L_{\rm IR} \geqslant 10^{11}\,{\rm L}_{\odot}$; LIRGs) are dusty, strong IR emitters where an enhancement of star formation is taking place (for references see Lípari et al. 2000); and imaging surveys of ultraluminous IR galaxies ($L_{\rm IR} \geqslant 10^{12}\,{\rm L}_{\odot}$; ULIRGs) show that ∼100 per cent are mergers or strongly interacting systems (Sanders et al. 1988a; Melnick & Mirabel 1990; Clements et al. 1996). There is compelling evidence of merger-driven starburst and nuclear activity; probably by deposition of large amounts of interstellar gas into the nuclear regions (see Scoville & Soifer 1991; Barnes & Hernquist 1992; Mihos & Hernquist 1994a,b, 1996; Sanders & Mirabel 1996). In addition, galactic winds, bubbles and Wolf–Rayet features have been clearly detected, in both starburst and IR galaxies (for references see Heckman, Armus & Miley 1990; Lípari & Macchetto 1992).

The discovery and study of luminous IR QSOs and IR-selected QSOs (see Beichman et al. 1986; Vader et al. 1987; Lawrence et al. 1988; Sanders et al. 1988b; Low et al. 1988, 1989; Lípari, Macchetto & Golombeck 1991; Colina, Lípari & Macchetto 1991b; Lípari, Colina & Macchetto 1994; and others) raises several interesting questions, in particular: are they a new or a special class of QSOs? In the last years, it has been proposed that luminous IR QSOs are normal AGNs, merely viewed at particular angles (Wills et al. 1992; Hines & Wills 1995; Boyce et al. 1996). While this hypothesis is interesting, it has problems explaining several observational results (Canalizo, Stockton & Roth 1998). On the other hand, we found that almost 100 per cent of extremely strong Fe II emitters are luminous IR QSOs and are radio-quiet. We suggested that these objects could be young IR active galaxies at the end phase of a strong starburst (Lípari, Terlevich & Macchetto 1993). In recent years, composite models (non-thermal – AGN plus starburst/superwind scenario) have become a widely accepted approach in studying the source of nuclear energy in IR galaxies and QSOs (see Genzel et al. 1998; Downes & Solomon 1998; Veilleux, Kim & Sanders 1999; Taniguchi et al. 1999a; Lutz, Veilleux & Genzel 1999; Smith et al. 1998).

Some of the results obtained for low-ionization BAL QSOs, such as very weak [O III] λ5007 emission, strong blue asymmetry in Hα, radio quietness and strong IR and Fe II emission (Boroson & Meyers 1992; Lípari et al. 1993), can also be explained within the framework of the starburst+AGN scenario. In our study of Mrk 231 and IRAS 0759+6559 (the nearest extreme Fe II IR and BAL systems), we detected typical characteristics of young-starburst QSOs and found evidence of a probable link between BAL systems and star formation regions. Specifically, our evolutive model for young IR QSOs (for references see Lípari 1994) suggested that BAL systems could be linked to violent supermassive starburst that can lead to a large-scale expanding shell and is often obscured by dust. Several articles recently suggested that this evolutive model shows good agreement with the observations (see Canalizo & Stockton 1997; Lawrence et al. 1997; Canalizo et al. 1998).

Over the last few years, several possible links between mergers, starbursts and IR QSOs have been proposed. Specifically, Joseph et al., Sanders et al. and Lípari et al. suggested three complementary sequences and evolutive links:

(i) merger → giant shocks → super-starbursts + galactic winds → elliptical galaxies;

(ii) merger → H_2-inflow (starbursts) → cold ULIRGs → warm ULIRGs + QSOs;

(iii) merger/s → extreme starburst + galactic wind (inflow + outflow) → Fe II/BAL composite IR-QSOs → standard QSOs and ellipticals.

High-resolution studies of nearby IR mergers and IR QSO are one observational way of studying these relations. We have started a detailed morphological, spectroscopic and kinematic study of these kinds of objects (see Lípari et al. 2000 for references); and we introduce several selected results from this programme. In this paper we analyse the outflow (OF) and/or Wolf–Rayet (WR) features in: (i) two nearby mergers, 'the Antennae' ($z = 0.0056$, $L_{\rm IR[8-1000\,\mu m]} \sim 1.0 \times 10^{11}\,{\rm L}_{\odot}$); and IRAS 23128−5919 ($z = 0.0449$, $L_{\rm IR[8-1000\,\mu m]} = 2.0 \times 10^{12}\,{\rm L}_{\odot}$); (ii) two relatively nearby IR QSOs, IRAS 01003−2238 ($z = 0.1180$, $L_{\rm IR[8-1000\,\mu m]} = 1.74 \times 10^{12}\,{\rm L}_{\odot}$) and IRAS 13218+0552 ($z = 0.2048$, $L_{\rm IR[8-1000\,\mu m]} = 4.26 \times 10^{12}\,{\rm L}_{\odot}$; Armus, Heckman & Miley 1988; Sanders et al. 1988b; Low et al. 1988, 1989; Remillard et al. 1993); and (iii) in the large sample of ultraluminous IR galaxies/QSOs ('The IRAS 1-Jy Survey'; Kim & Sanders 1998; Kim et al. 1998; Veilleux et al. 1999) and bright PG-QSOs (Boroson & Green 1992). Throughout the paper, a Hubble constant of $H_0 = 75$ km s^{-1} Mpc^{-1} will be assumed.

2 OBSERVATIONS AND REDUCTIONS

The observations were performed at the European Southern Observatory (ESO), Complejo Astronómico El Leoncito (CASLEO) and Bosque Alegre Station (BALEGRE); with the 3.6–3.5-, 2.15- and 1.54-m telescopes, respectively. We also used spectra obtained by Veilleux et al. (1999) and Boroson & Green (1992) at Kitt Peak National Observatory (KPNO) and Mauna Kea Observatory (MKO); with the 2.15- and 2.2-m telescopes, respectively. In addition, *HST* WFPC2 archive images were studied. Table 1 shows a summary of the observations analysed in this paper.

The ESO Faint Object Spectrograph and Camera (EFOSC) on the 3.6- and NTT 3.5-m telescopes at La Silla was used to obtain long-slit spectra and high-resolution broad and narrow-band images (during three photometric nights in 1995 January, 1991 August and 1990 August). Medium-resolution spectra were obtained with the B150, O150 and R150 grisms, which provide a resolution of ∼7 Å in the wavelength range 3600–9800 Å. Images through broad-band (V, R) and interference (Hα+[N II]) filters were obtained. The seeing was in the range 0.8–2.0 arcsec (FWHM).

Long-slit spectroscopic observations were performed at the 2.15-m telescope of CASLEO during the period 1999 December to 2001 June. The spectra with moderate resolution were obtained with the University of Columbia spectrograph (Lípari, Tsvetanov & Macchetto 1997). The observations were made using a slit width of 2 arcsec, which gave an effective resolution of ∼7 Å (∼280 km s^{-1}), in the wavelength range 3600–7000 Å. The observing conditions were photometric, and the seeing was in the range 1.5–2.8 arcsec (FWHM).

Long-slit spectroscopic observations were obtained at the 1.54-m telescope of BALEGRE Station of Cordoba Observatory using the Multifunctional Integral Field Spectrograph (Afanasiev, Dodonov & Carranza 1994; Díaz et al. 1999) during five photometric nights between 1998 May and 2000 May. The observations were made

Table 1. Journal of new and archival observations.

Object	Date	Telescope/ instrument	Spectral region	Expos. time (s)	Comments
NGC 4038/39	1998 May 29	BALEGRE 1.54 m	λλ6400–6900	1800 × 6	PA 174° long-slit = 1 arcsec
NGC 4039	1999 Jan 14		λλ6400–6900	1800 × 4	PA 10°, PA 65°
	2000 Feb 09		λλ6400–6900	1800 × 4	PA 125°
	2000 Feb 27		λλ6400–6900	1800 × 4	PA 20°
	2000 May 6		λλ6400–6900	1800 × 4	PA 90°, PA 175°
NGC 4038/39	2000 May 24	CASLEO 2.15 m	λλ4000–7500	1800 × 2	PA 174° long-slit = 1.5 arcsec
	2000 May 25		λλ4000–7500	1800 × 2	PA 174° long-slit = 1.5 arcsec
NGC 4038/39	1991 Aug 29	ESO EFOSC 3.6 m	λλ3600–5590	1200 × 2	PA 174° long-slit = 1.5 arcsec
			λλ5050–7000	1200 × 2	PA 174°
			λλ6600–9800	1200 × 2	PA 174°
I23128–5919	1999 Dec 08	CASLEO 2.15 m	λλ3600–6900	1800 × 2	PA 90° long-slit = 1.5 arcsec
			λλ3600–6900	1800 × 2	PA 76°
	1997 Mar 14	*HST*/WFPC2	F702W, λλ6895/1389	1800	
I01003−2238	1995 Oct 26	KPNO 2.15 m	λλ4570–8960	1800	PA 00° long-slit = 2 arcsec
	1995 Oct 21	*HST*/WFPC2	F814W, λλ7970/1531	1000	
	1995 Mar 22	*HST*/WFPC2	F439W, λλ4300/475	2800	
I13218+0552	1993 Apr 01	MKO 2.2 m	λλ5650–8770	1800	PA 90° long-slit = 2 arcsec
	1994 Dec 11	*HST*/WFPC2	F702W, λλ6895/1389	1800	
I11119+3257	1993 May 15	MKO 2.2 m	λλ4820–8170	1000	PA 90° long-slit = 2 arcsec
I14394+5332	1992 Jul 07	MKO 2.2 m	λλ4725–7740	600	PA 90°
I15130–1958	1992 Jul 07	MKO 2.2 m	λλ4750–7770	600	PA 90°
I15462–0450	1995 Mar 28	MKO 2.2 m	λλ4710–8990	1800	PA 90°
I05024–1941	1995 Oct 26	KPNO 2.15 m	λλ4570–8970	2700	PA 00°
I13305–1739	1995 Mar 26	KPNO 2.15 m	λλ4710–8980	1800	PA 00°
I13451+1232	1993 May 14	MKO 2.2 m	λλ4820–7880	700	PA 90°
I23389+0303	1995 Oct 27	KPNO 2.15 m	λλ4570–8970	2700	PA 00°
PG 1444+407	1991 Apr 23	KPNO 2.15 m	λλ4300–5700	3000	PA 00° long-slit = 1.5 arcsec
PG 1448+273	1990 Feb 15	KPNO 2.15 m	λλ4300–5700	1350	PA 00°
PG 1244+026	1990 Feb 15	KPNO 2.15 m	λλ4300–5700	3200	PA 00°
PG 1535+547	1990 Feb 15	KPNO 2.15 m	λλ4300–5700	1400	PA 00°
I07598+6508	1995 Nov 07	*HST*/WFPC2	F702W, λλ6895/1389	1800	
Mrk 231	1995 Oct 23	*HST*/WFPC2	F814W, λλ7970/1531	712	
			F439W, λλ4300/475	2226	
I14026+4341	1994 May 30	*HST*/WFPC2	F702W, λλ6895/1389	560	
			F555W, λλ5407/1236	3200	
I17002+5153	1998 Jul 20	*HST*/WFPC2	F547M, λλ5479/486	2240	
	1990 Sep 19	KPNO 2.15 m	λλ4300–5700	2400	
I04505−2958	1995 Sep 30	*HST*/WFPC2	F702W, λλ6895/1389	1800	
	1999 Dec 8	CASLEO 2.15 m	λλ4300–7700	1800 × 2	PA 90° long-slit = 1.5 arcsec
I00275−2859	1996 Oct 05	*HST*/WFPC2	F814W, λλ7970/1531	800	
	1995 Jan 07	ESO EFOSC 3.6 m	λλ3600–5590	1200 × 2	PA 90° long-slit = 1.5 arcsec
			λλ5050–7000	1200 × 2	
I13349+2438	1997 May 13	*HST*/WFPC2	F814W, λλ7970/1531	800	
I Zw 1	1996 Aug 29	*HST*/WFPC2	F814W, λλ7970/1531	800	
	1999 Dec 8	CASLEO 2.15 m	λλ4300–7700	1800 × 2	PA 90° long-slit = 1.5 arcsec
I19254–7245	1996 Mar 04	*HST*/WFPC2	F814W, λλ7970/1531	800	
	1997 Mar 27	*HST*/WFPC2	F814W, λλ7970/1531	400	
	1990 Aug 20	ESO EFOSC2 3.5 m (NTT)	E442 λλ6955/95	600 × 2	Hα redshifted
			E629λλ6571/115	600 × 2	Hα continuum
			E584 V	400 × 2	
			E585 R	400 × 2	
	2001 Jun 25	CASLEO 2.15 m	λλ4000–7300	1800 × 2	PA 175° long-slit = 1.5 arcsec
	2001 Jun 27		λλ4000–7300	1800 × 2	PA 175°

Note: The new observations are those obtained at ESO, CASLEO and BALEGRE observatories.

mainly with a slit width of 1.0 arcsec and a 1200 groove mm^{-1} grating, which gave an effective resolution of ∼90 km s^{-1} covering the wavelength range 6400–6900 Å. In order to have accurate spatial positions for the velocity determinations, zeroth-order images of object plus slit were used. The seeing was in the range 1.3–2.5 arcsec (FWHM).

The *HST* WFPC2 archival observations include broad-band images positioned mainly on the Planetary Camera (PC) chip with a

pixel scale of 0.046 arcsec pixel^{-1}, and using the filters F439W, F450W ($\sim B$ Cousins filter), F547M, F555W, F606W, F702W and F814W ($\sim I$); see Table 1.

We used the spectra of the *IRAS* 1-Jy ULIRGs sample (Kim & Sanders 1998; Veilleux et al. 1999), which were obtained with the Gold Cam Spectrograph on the KPNO 2.15-m telescope using a grating of 300 line mm^{-1} (8.3-Å resolution, in the wavelength range ~4500–9000 Å); and with the Faint Object Spectrograph of the University of Hawaii 2.2-m telescope at MKO, at the $f/10$ Cassegrain focus, using a grating of 600 line mm^{-1} (8.3-Å resolution, in the wavelength range ~4700–9000 Å).

We also used the spectra of the PG QSOs sample (Boroson & Green 1992), which were obtained with the Gold Cam Spectrograph on the KPNO 2.15-m telescope using two gratings of 300 grooves mm^{-1} (8 Å resolution, covering the rest wavelength range 4300–5700 Å). We have digitized the published spectra of IRAS 01003−2238 and 13218+0552 (from Armus et al. 1988 and Remillard et al. 1993, respectively).

The IRAF,[2] SAO[3] and ADHOC[4] software packages were used to reduce the data. Bias and dark subtraction and flat-fielding were performed in the usual way. Wavelength calibration of the spectra was carried out by fitting two-dimensional polynomials to the position of lines in the arc frame. The spectra were corrected for atmospheric extinction, galactic reddening and redshift. The spectra were flux calibrated using observations of standard stars from the samples of Stone & Baldwin (1983).

3 RESULTS

This section focuses on presenting spectroscopic and/or morphological evidence of outflow and WR features in nearby IR mergers and IR QSOs (where previously starburst, bipolar extended emission, etc. were detected). In addition, we analyse: (i) EVOF in the IRAS 1-Jy ULIRG sample; (ii) the host galaxies of IR QSOs (using high-resolution *HST* images); and (iii) the presence of Wolf–Rayet features in part of the sample of bright PG QSOs.

The evidence of OF in nearby objects are kinematic, morphological and physical (see Heckman et al. 1990). However, for distant galaxies and QSOs this evidence is mainly the presence of high-velocity components in the kinematic data. These high values of velocity could only be associated with OF, since the other possible processes (such as tidal disruption) show mostly low-velocity values, as we observed in the velocity field of nearby mergers and galaxies ($|v| < 300$ km s^{-1}, e.g. Lípari et al. 2000).

The high-velocity emission-line components were measured and decomposed using Gaussian profiles by means of a non-linear least-square algorithm described in Bevington (1969). In particular, the high-velocity components were measured: (i) at least in two different emission lines, for each spectrum and (ii) at least in two different spectra, for each object (mainly in the case of a nearby IR merger/QSO). Therefore, in order to 'verify' the high-velocity components detection we observed each object several times and we also digitized published spectra (see Table 1 and Section 2).

In this paper, we define the limit between EVOF and low-velocity OF at 700 km s^{-1}, that is $V_{\rm EVOF} > 700$ km s^{-1} $\geqslant V_{\rm lvOF}$ (based in the results obtained in this and a previous paper: for details see Sections 4.1 and 4.2, and Lípari 1994; Lípari et al. 2000). In addition, we note that in nearby objects we measure the OF components relative to the systemic velocity; however, for distant galaxies/QSOs we measure the OF mainly from the main emission-line component (since the systemic velocity is frequently not available).

3.1 Nuclear outflow and WR features in nearby mergers: 'The Antennae' and IRAS 23128−5919

As we noted in Section 1, we have started a detailed morphological, spectroscopic and kinematic study of nearby IR mergers and IR QSO; especially those with starburst and galactic winds (or candidates; see Lípari et al. 1994, 2000). This programme includes the study of NGC 4038/39, 3256, Arp 220, Mrk 231, NGC 2623, IRAS 01003−2238, 07598+6508, 13218+0552, 17002+5153, 19254−7245, I Zw 1, PHL 1092 and others. The OF and WR detections for two nearby IR mergers and two IR QSOs are summarized in Tables 2 and 3, respectively.

Read, Ponman & Wolstencroft (1995) and Fabbiano, Schweizer & Mackie (1997) already suggested the presence of outflow in The Antennae, from X-ray observations. Rosa & D'Oddorico (1986) also suggested the presence of WR features in the H II regions of the Antennae. In order to detect the OF component in the nuclear region of NGC 4038/39, long-exposure spectroscopic observations were performed at BALEGRE (resolution of ~90 km s^{-1} covering the wavelength range 6400–6900 Å) with a total integration time of ~3 h. The spectra were taken mainly through both nuclei. In the southern nucleus (NGC 4039) we found a defined blue component in Hα and [N II] λ6584 emission lines (Fig. 1a). The velocity of this nuclear outflow is $V_{\rm nucl\,OF} = (-365 \pm 50)$ km s^{-1}. This OF component was detected at signal-to-noise (S/N) ratio ~ 4. In Section 4 this component will be associated with the nuclear starburst, detected previously in the nucleus of NGC 4039. This blue outflow component (with relatively low velocity) was clearly detected only using data of moderate/high spectral resolution (~90 km s^{-1} FWHM) and high S/N ratio.

ESO and CASLEO spectra (resolution of ~300 km s^{-1}, covering the wavelength range 3600–9800 and 4000–7500 Å, respectively) of the NGC 4039 nucleus show LINER properties. The values of the emission-line ratios: [O I] λ6300/Hα = 0.13, [O I] λ6300/[O III] λ5007 = 0.53, [O III] λ5007/Hβ = 0.94, [N II] λ6584/Hα = 0.47 and [S II] λ6517-31/Hα = 0.56 are clearly consistent with shocks driven into clouds accelerated outwards by a starburst with galactic wind (see Lípari et al., in preparation; Heckman et al. 1990, their fig. 14). The nucleus of NGC 4038 shows H II region characteristics.

The presence of outflow in the nuclear region of IRAS 23128−5919 has been previously suggested by Bergvall & Johansson (1985) and Johansson & Bergvall (1988); in addition they found – in this region – WR features. We detected, using CASLEO spectra (resolution of ~300 km s^{-1}), low-velocity outflow and WR features in the bright southern nucleus of IRAS 23128−5919, with a value of $V_{\rm nucl\,OF} = (-300 \pm 70)$ km s^{-1}. We detected this OF component at low S/N ratio (~2); since this OF feature is very weak (therefore, a new study with better spectral resolution is required).

Fig. 6(c) (see Section 3.4) displays the high-resolution *HST* WFPC2 image (through filter F814W) of the merger IRAS 23128−5919, featured by two faint tails and the main body of the merger. Inside of this main body, the morphology is very similar to The Antennae, i.e. two distorted discs in the early phase of a merger process; with two nuclei surrounded by bright knots (probably associated with massive star formation processes). Bergvall & Johansson (1985) and Johansson & Bergvall (1988) found

[2] IRAF is the imaging analysis software facility developed by NOAO.

[3] SAO is the imaging analysis software developed by the Special Astrophysical Observatory, Russian Academy of Sciences.

[4] ADHOC is the imaging analysis software developed by Marseilles Observatory.

Table 2. Nuclear outflow and WR features in nearby mergers.

Object	V_{OF} (km s^{-1})	z	L_{IR} (log $L_{IR}/L_{\odot}$)	Type	WR	Comments
NGC 4039	-365 ± 50	0.0056	11.0	L+SB	Yes	OF Hα and [N II] λ6584
IRAS 23128−5919	-300 ± 70	0.0449	12.6	L+SB	Yes	southern nucleus OF Hα and [N II]

Note: L: Liners and SB: starburst.

Table 3. Extreme velocity outflow in IR QSOs/AGNs.

Object (*IRAS*)	V_{OF1} (km s^{-1})	V_{OF2} (km s^{-1})	z	L_{IR} (log $L_{IR}/L_{\odot}$)	Type	WR	Comments
01003−2230	−770	−1520	0.1180	12.24	QSO+SB	Yes	OF [O III], Hβ
13218+0552	−1800	(−3438)	0.2048	12.63	QSO+SB	(Yes)	”
19254−7245	−800	–	0.0597	12.04	S2+SB	–	”
Mrk 231	−1000	–	0.0422	12.50	S1+SB	–	OF [O II]
11119+3257	−1300	(−2120)	0.1873	12.58	S1+SB	(Yes)	OF [O III]
14394+5332	−880	(−1650)	0.1050	12.04	S2	–	OF [O III], Hβ
15130–1958	−780	(−1200)	0.1093	12.09	S2	–	OF [O III]
15462–0450	−1000	(−1760)	0.1001	12.16	S1	–	”

Note: The uncertainties are $e(V_{OF}) \sim \pm 100$ km s^{-1} and $e(z) \sim \pm 0.0002$. Values in parentheses are possible detections. S1: Seyfert 1 and S2: Seyfert 2.

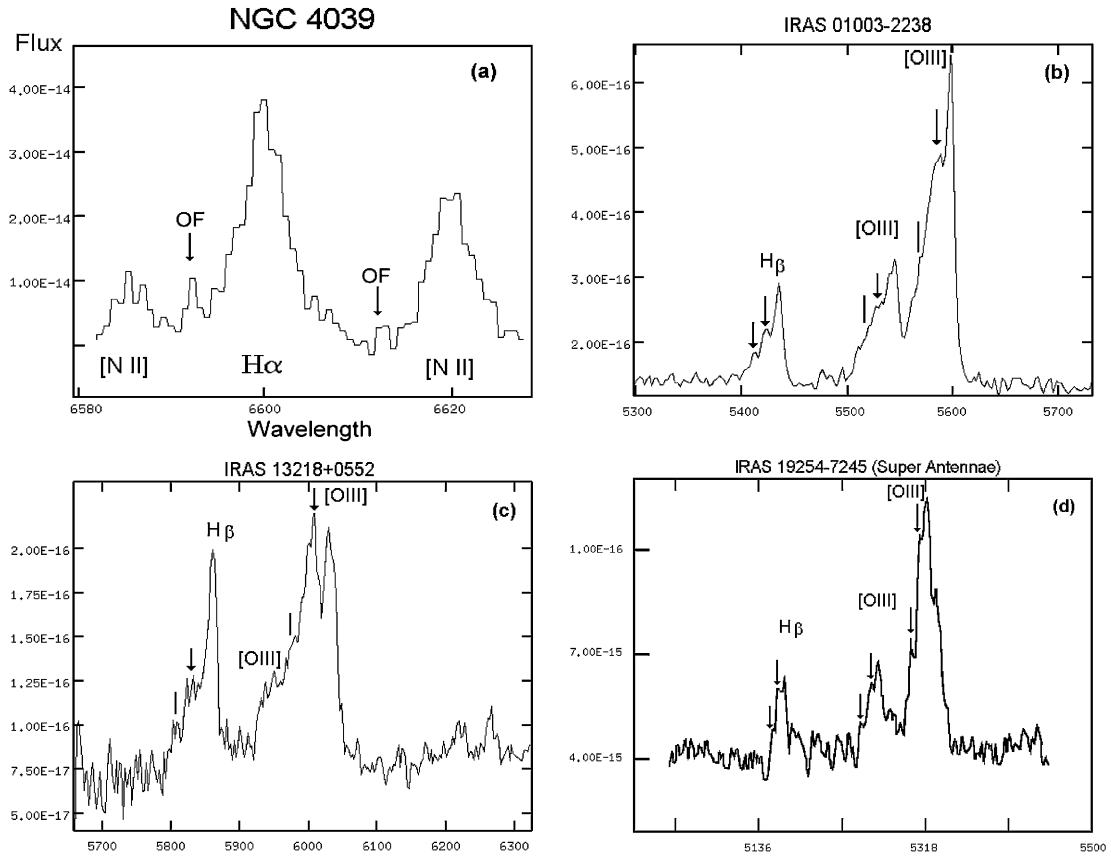

Figure 1. (a) BALEGRE optical spectrum of NGC 4039 in the Hα+[N II] $\lambda\lambda$6548,6583 region (along PA 174°, through the nucleus). It shows the OF nuclear component. (b)–(d) MKO optical spectra of the QSOs IRAS 01003−2238, 13218+0552 and CASLEO spectrum of IRAS 19254−7245. They show the EVOF components in the Hβ+[O III] $\lambda\lambda$4959,5007 region. The arrows show confirmed OF features and vertical bars show possible OF (see the text).

in the spectra of the nuclear region of IRAS 23128−5919 LINER+starburst features, and they suggested that the nuclear emission-line ratios are consistent with shocks associated with a starburst with galactic wind (i.e. to supernova (SN) explosions). Using CASLEO spectra (of IRAS 23128−5919) we found in the southern nucleus strong stellar absorption features at Hδ, H7, H8 and H9; and the following values for the emission-line ratios: [O II] λ3727/[O III] λ5007 = 0.87, [O I] λ6300/[O III] λ5007 = 0.14, [O I] λ6300/Hα = 0.09, [O III] λ5007/Hβ = 2.78, [N II] λ6584/Hα = 0.38 and [S II] λ6517-31/Hα = 0.32; these results are in agreement with the starburst+galactic-wind scenario proposed by Johansson & Bergvall (1988). The northern nucleus (of IRAS 23128−5919) shows emission-line ratios in the range of H II regions to LINERs.

3.2 Outflow and WR features in the nearby IR QSOs: IRAS 01003−2238 and 13218+0552

IRAS 01003−2238 and 13218+0552 are probably two of the more interesting IR QSOs. In IRAS 01003−2238, Armus et al. (1988) found for the first time clear WR features in a QSO. IRAS 13218+0552 has a ratio $L_{\rm IR}/L_{\rm OPT}$ of 91.0, much higher than the median for IR and PG QSOs (6.1 and 2.1, respectively; Low et al. 1989); this ratio make this object one of the reddest QSOs known. In their optical spectra, obtained at KPNO and MKO (resolution of ∼300 km s^{-1}), we detected EVOF components, mainly in the [O III] $\lambda\lambda$5007–4959 and Hβ emission lines (Figs 1b and c). We measured for IRAS 01003−2238 outflow velocities of $V_{\rm OF1}$ = (−770 ± 50) km s^{-1} and $V_{\rm OF2}$ = (−1520 ± 60) km s^{-1}, and for the main emission-line component, a value of $z_{\rm MELC} = 0.1180$. These OF components were clearly detected at S/N ∼ 7 and 4 (for OF1 and OF2, respectively). For IRAS 13218+0552 we have obtained $V_{\rm OF}$ = (−1800 ± 90) km s^{-1} and $z_{\rm MELC} = 0.2048$. We observed this OF component at S/N ∼ 4. In the Hβ emission line we detected a possible second OF component (S/N ∼ 2; see Table 3); however, this feature needs to be confirmed. Fig. 2 depicts an example of Gaussian deblending and the measure of high-velocity components, in IRAS 01003−2238.

We note that in both IR QSOs the high-velocity components reported as detections were confirmed first by detecting each component in two or three different emission lines ([O III] λ5007, [O III] λ4959 and/or Hβ) in the KPNO and MKO spectra; and also measuring the high-velocity components in our digitized spectra of IRAS 01003−2238 and 13218+0552 (from Armus et al. 1988; Remillard et al. 1993, respectively). These high-velocity values observed, allowed us to associate these features only to OF processes (see the introduction of Section 3).

The *HST* WFPC2 images of IRAS 01003−2238 (through the filter F814W) and 13218+0552 (through F702W) display interesting features, as seen in Figs 6(b)–(d). IRAS 01003−2238 has a point-like image with a small extension to the east. In this extension Surace et al. (1998) found a chain/arc of five extremely blue and young starburst knots; which is consistent with the detection of WR features. This chain of blue knots is similar to those reported in the blue arc of Mrk 231 (see Section 3.4 for details). Furthermore, this chain structure also resembles the arc of nine extremely blue young starburst knots, found by Conti & Vacca (1994) in He 2–10, one of the nearest WR galaxies. The *HST* image of IRAS 13218+0552 depicts the host galaxy with a clear external loop/arcs (to the north of the nucleus) plus a faint tidal tail; these two features are probably associated with a merger process.

We have detected possible weak WR features in IRAS 13218+0552 (at S/N ∼ 2, requiring a confirmation with spectra of better resolution and S/N ratio). Therefore, these two IR QSOs probably have a composite nature as the source of nuclear

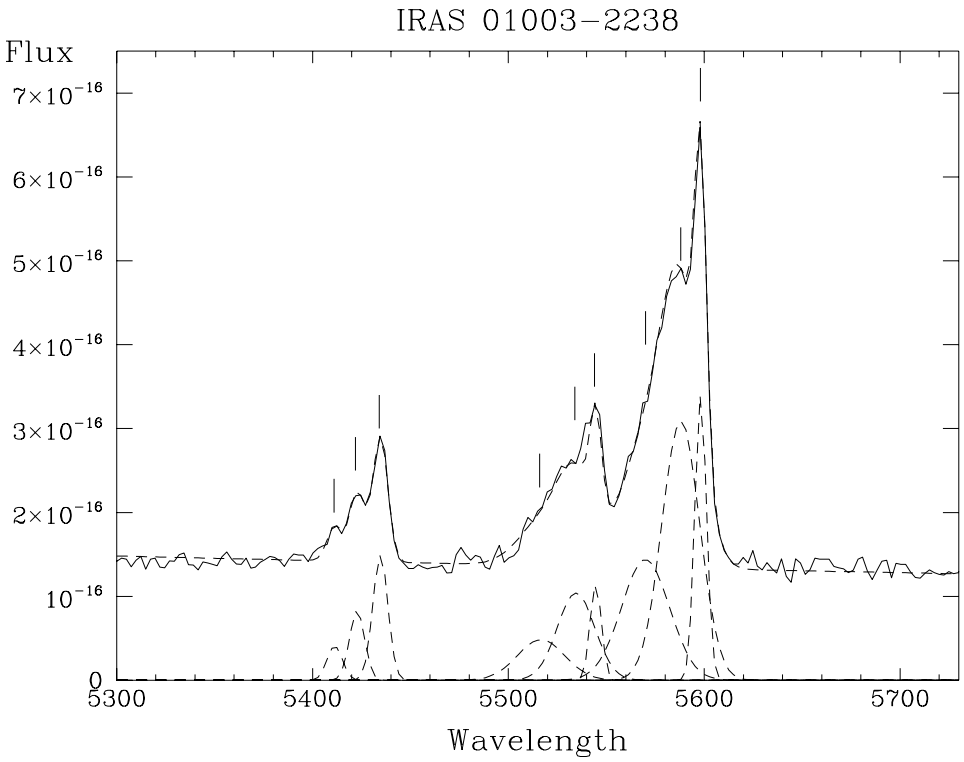

Figure 2. Deblending of high-velocity components in the spectrum of IRAS 01003−2238, at the wavelength region of Hβ and [O III] $\lambda\lambda$4959,5007. The dashed line shows the deblending fit.

energy. In Section 4 the EVOF components will be addressed mainly as being related to the coexistence of the starburst+QSO processes.

Note that we previously found similar OF results for two ULIRGs, i.e. EVOF in [O III], Hβ and [O II] emission lines. First, in the southern nucleus of the IR merger IRAS 19254−7245 ('The Super-Antennae', with $z = 0.059\,66$, $L_{\rm IR} = 1.1 \times 10^{12}\,{\rm L}_{\odot}$), we detected a massive starburst with a strong galactic wind and $V_{\rm OF} \sim -800$ km s^{-1}, plus a type II QSO (Colina, Lípari & Macchetto 1991a; see Fig. 1d). We also detected similar EVOF in Mrk 231 ($V_{\rm OF} \sim -1000$ km s^{-1}, in [O II]), this IR merger also has a strong circumnuclear starburst/galactic wind, plus an obscured type I QSO (Lípari et al. 1994). In Section 3.4 we present new interesting results of these two EVOF ULIRGs; and in Section 4.2 we comment the properties of EVOF objects.

3.3 Extreme outflow in ULIRGs: the IRAS 1-Jy sample

An interesting test in order to study the role of galactic wind in IR mergers and IR QSOs (and their relation), is the analysis of outflow in a complete sample of luminous IR Galaxies and QSOs. We analysed the spectra of the IRAS 1-Jy sample of ULIRGs (Kim & Sanders 1998; Kim et al. 1998; Veilleux et al. 1999), which is a flux-complete sample of 118 objects, obtained from the *IRAS* Faint Source Catalog, for flux$_{60\,\mu{\rm m}} \geqslant 1.0$ Jy (for $|b| > 30^{\circ}$ and $\delta > -40^{\circ}$).

The study of EVOF observed as high-velocity or multiple components in the emission line [O III] λ5007 requires in most cases, spectra with moderate spectral resolution (since these objects show very high FWHM([O III]) values). Therefore, we could perform a detailed search of EVOF, with FWHM([O III]) $\geqslant$1000 km s^{-1}, in the MKO-KPNO spectra survey of 1-Jy ULIRGs and IR QSOs. We found 11 objects that fulfil this criteria and several show OF components.

(i) We detected clear EVOF at [O III] and, when the line had a high enough S/N ratio, Hβ in IRAS 11119+3257, 14394+5332, 15130–1958 and 15462−0450 (see Table 3 and Fig. 3). The OF components were detected at a S/N ratio in the range ∼2–6. In addition, the spectrum of IRAS 11119+3257 shows (at S/N ∼ 2) possible WR features.

(ii) We found probable OF in IRAS 05024−1941, 13305−1739, 13451+1232 and 23389+0300; at a S/N ratio in the range ∼2–3. However, better spectral resolution and S/N ratios are required, in order to confirm the presence of OF in these objects.

(iii) The IR QSOs with EVOF IRAS 01003−2238 and 13218+0552 are also included in this IRAS 1-Jy sample.

(iv) For the remaining object (IRAS 21219−1757), the high values in the FWHM([O III]) are due mainly to the blend of [O III] and Fe II emission lines (this IR QSO is a strong Fe II emitter).

The OF values that still required confirmation (i.e. possible detections), are presented in parentheses in Table 3. In addition, Figs 1 and 3 show arrows and vertical bars indicating confirmed and possible OF components, respectively. We also note that the confirmed features are those with detections in two or three emission lines and with S/N $\geqslant$ 3.

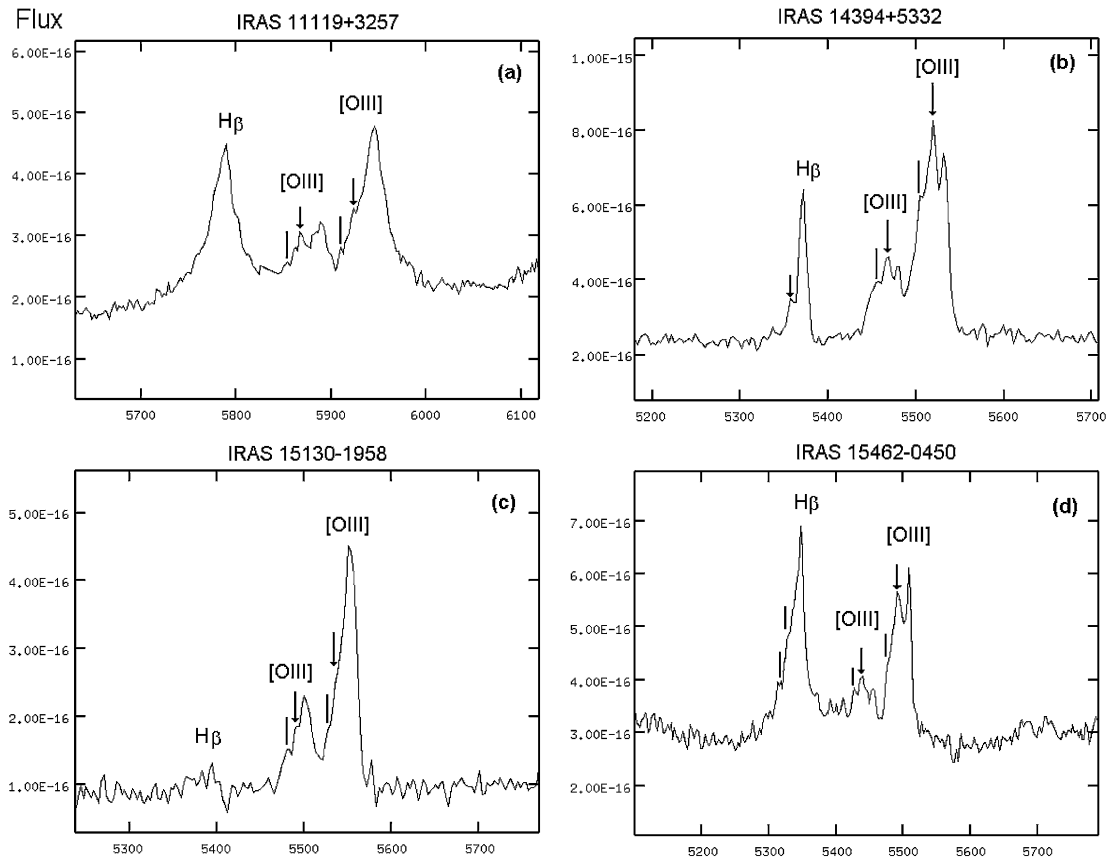

Figure 3. (a)–(d) MKO optical spectrum of IRAS 11119+3257, 14394−5332, 15130−1958 and 15462−0450. They show the EVOF components in the Hβ+[O III] $\lambda\lambda$4959,5007. The arrows show confirmed OF features and vertical bars possible OF.

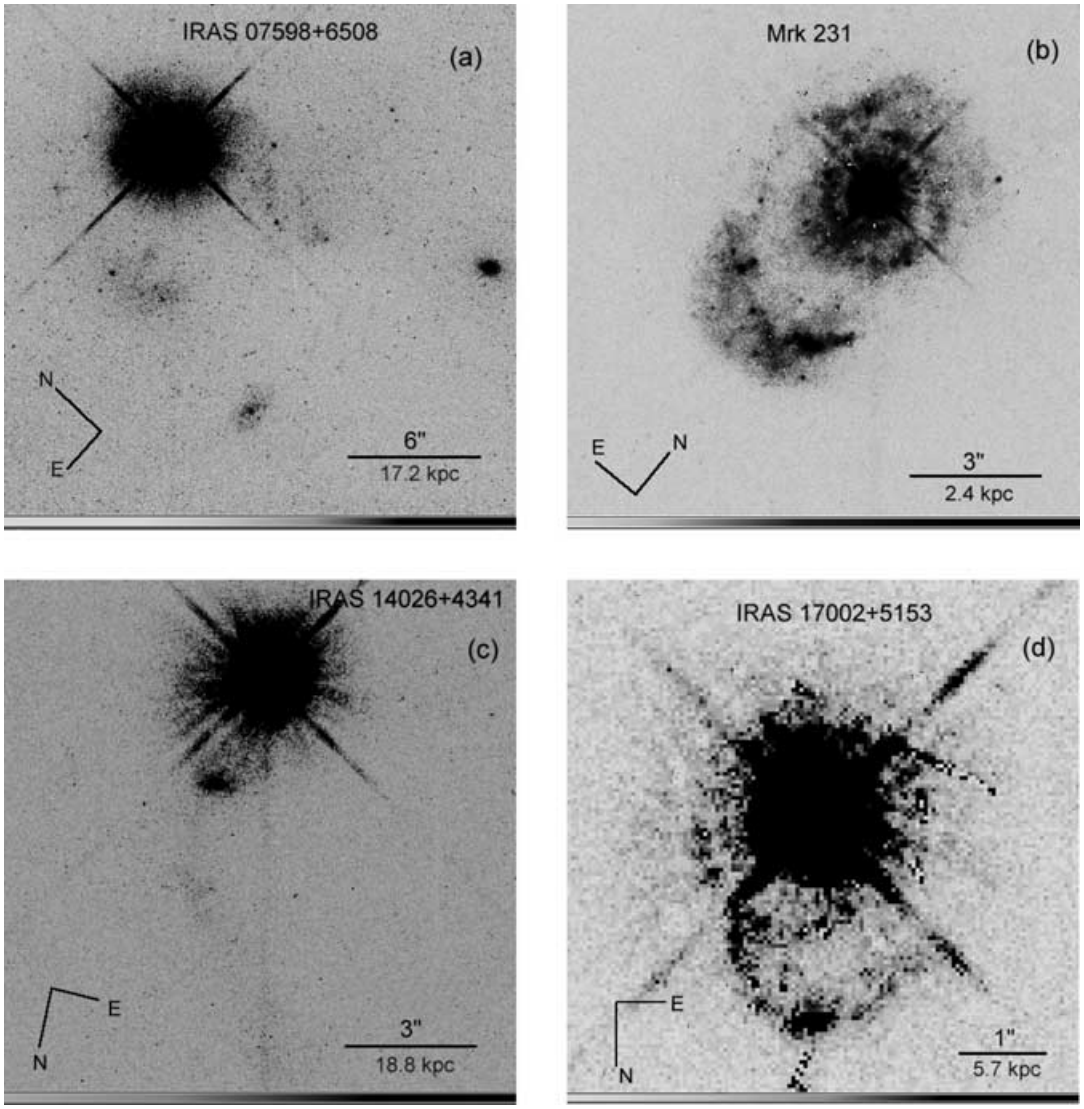

Figure 4. *HST* broad-band images of four strong IR QSOs which are BAL+Fe II QSOs. Note that all these IR objects show 'arcs or shells' and/or merger features. (a) IRAS 07598+6508 (through the filter F702W); (b) IRAS 12540+5708 (Mrk 231, through F439W); (c) IRAS 14026+4341 (through F702W); (d) IRAS/PG 1700+518 (through F547M).

3.4 Morphological evidence of outflow, arcs and bubbles in nearby IR mergers and IR/BAL QSOs

Figs 4 and 5 show broad-band high-resolution *HST* images of luminous IR QSOs (which are mainly strong BAL and Fe II QSOs; Low et al. 1989; Boroson & Meyers 1992; Lípari et al. 1993). We selected IR QSOs for which high-resolution *HST* images are available. All of these objects show filaments and arcs extending mostly from the circumnuclear regions ($r \sim 1$ kpc) up to tens of kpc scales in some cases. The narrowness and curving structure of all the filaments clearly suggests confinement, although it is unclear whether the material is confined in one dimension or two, making it difficult to distinguish between bubbles, cones or ring cases. In addition, previous studies of high-resolution *HST* images of IR-selected BAL QSOs have also shown in practically all of these objects the presence of arcs or shells (Boyce et al. 1996; Stockton, Canalizo & Close 1998; Surace et al. 1998; Hines et al. 1999) very similar to those observed in Mrk 231 (the nearest IR merger with GW+Fe II+BAL QSO; Lípari et al. 1994) and in Arp 220 (the nearest IR merger with GW; Heckman, Armus & Miley 1987).

These 'circumnuclear and external arcs' could be associated mainly with the results of galaxy collision (tidal tails, rings, loops, etc.) or to the final phase of the galactic wind, i.e. the blowout phase of the galactic bubbles (Tomisaka & Ikeuchi 1988; Norman & Ikeuchi 1989; Suchkov et al. 1994). However, for distant AGNs and QSOs it is difficult to discriminate between these two related alternatives. Even for low-redshift BAL IR QSOs (such as Mrk 231) there are different interpretations concerning the origin of these 'blue arcs'. In particular, Lípari et al. (1994) found clear evidence of a powerful nuclear starburst with galactic wind in the circumnuclear region of Mrk 231, and we proposed a galactic-wind scenario for the origin of a blue arc, detected in this system ($r \sim 3.5$ kpc; Fig. 4b). However, Armus et al. (1994) suggested that this arc originated in the interaction between the main and an obscured nucleus (they also suggested that in this blue region and 'shell' there is no evidence of a star formation process). However, *HST* WFPC2 observations of Mrk 231 confirmed that this blue arc is a 'dense shell of star-forming knots' (Surace et al. 1998, see their figs 6 and 7). In addition, these *HST* WFPC2 F439W and F814W broad-band images (see Fig. 4b,

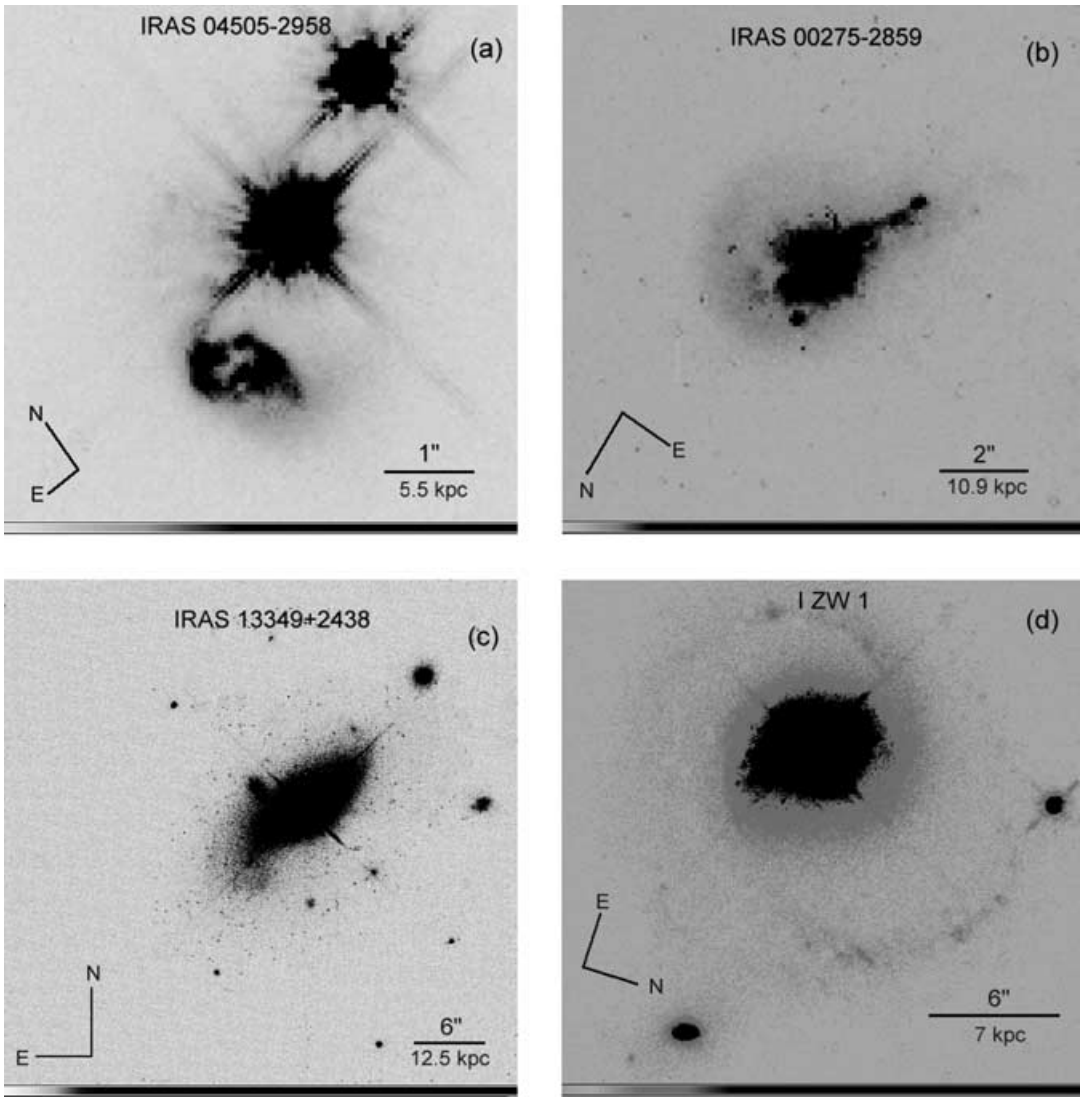

Figure 5. *HST* broad-band images of four strong IR QSOs which are strong Fe II emitters. Note that all these IR objects show 'arcs or shells' and/or merger features. (a) IRAS 04505−2958 (through the filter F702W); (b) IRAS 00275−2859 (through F814W); (c) IRAS 13349+2438 (through F814W); (d) I ZW 1 (through F814W).

and the colour map of Surace et al. 1998: their fig. 6) show blue spiral arms in the circumnuclear region of Mrk 231 ($r \sim 1.5$ kpc), similar to those observed in the central region of NGC 3256 (Lípari et al. 2000).

For the four selected IR QSOs, showing BAL+Fe II systems (Fig. 4), the *HST* WFPC2 high-resolution data suggest that the observed arcs or shells could be related mainly: (i) in Mrk 231, to star formation and outflowing material; (ii) in IRAS 07598+6508, to strong collision/merger process; while (iii) in PG/IRAS 17002+5153 and IRAS 14026+4341, it is not clear (Lípari et al., in preparation).

We note that in this morphological study of arcs, loops and shell structures, our intention is to combine the *HST* high-resolution data, colours maps (if they are available) and spectroscopic observations. Furthermore, recently we have obtained two-dimensional high-resolution spectroscopy (2 Å resolution) for Mrk 231, Arp 220, NGC 3690 and others (with the William Herschel 4.2-m telescope, at La Palma) in order to also include new detailed maps of the kinematic, emission lines, emission-line ratios and continuum (of these nearby IR mergers and IR QSOs; Lípari, Mediavilla & Diaz 2001). These maps will help to study in detail these two types of arcs: those associated with outflowing 'shocked' material and with tidal loops/tails in galactic collisions.

For the four IR QSOs with strong Fe II emission (Fig. 5), the *HST* WFPC2 morphological data suggest that (i) IRAS 04505−2958 has a very interesting feature, i.e. one of the clearest large-scale external arcs (Boyce et al. 1996) with an extension of ∼20 kpc!, which could be associated mainly with an OF process (the CASLEO spectra of this object do not show clear OF components, possibly as a result of blending with the Fe II emission); (ii) IRAS 00275−2859 displays a disrupted merger morphology; (iii) IRAS 13349+2438 shows a clear tidal tail, probably associated with a collision process; while (iv) I Zw 1 shows the bright nucleus, two spirals arms, plus the western companion galaxy; Schinnerer, Eckart & Tacconi (1998) found that the disc of I Zw 1 and the companion have a strong blue colour, suggesting that the star formation is enhanced in both galaxies.

In addition, for the nearby merger with EVOF IRAS 19254−7245 ('the Super-Antennae'), new *HST* WFPC2 broad-band images taken with the F814W filter (Fig. 6a) show a complete arc around the

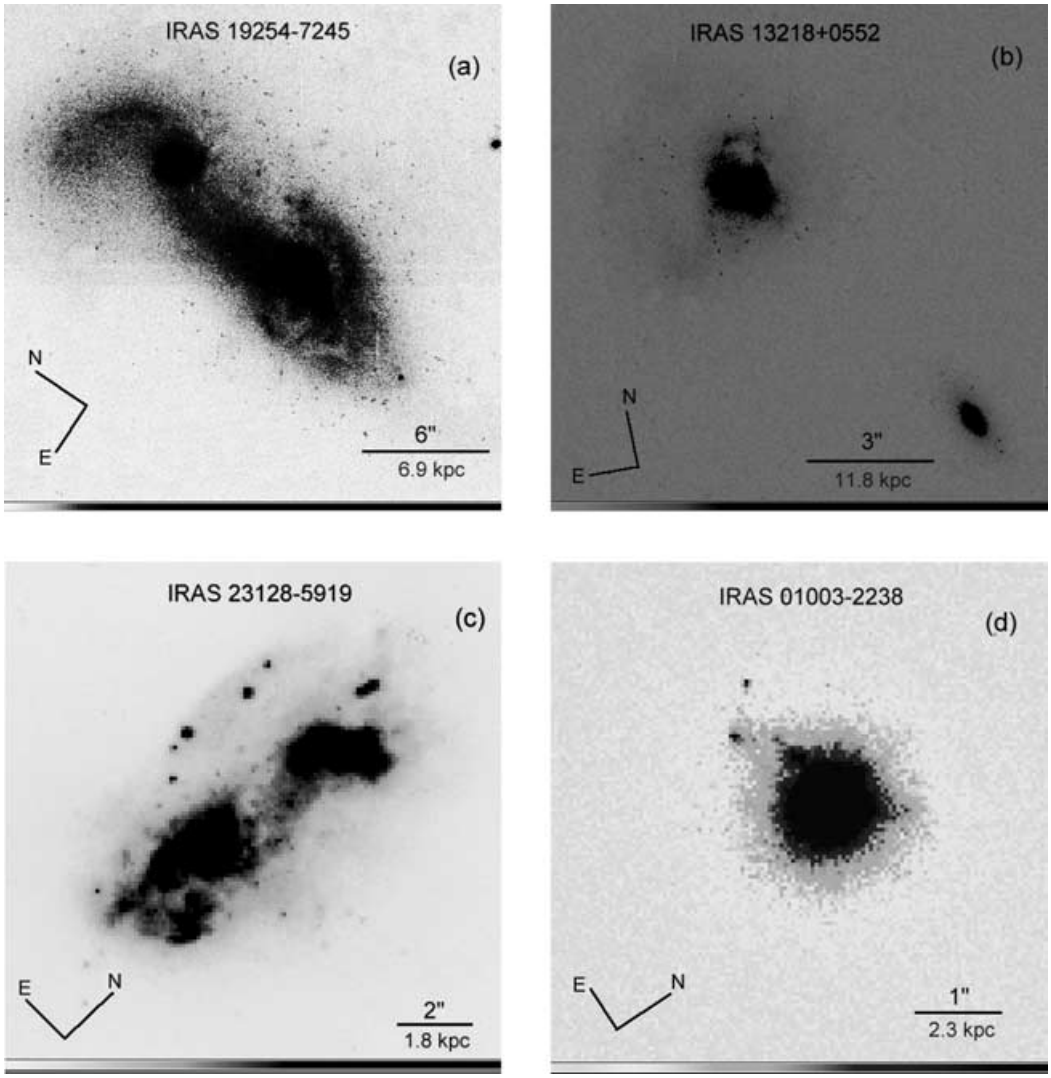

Figure 6. *HST* broad-band images of luminous IR QSOs and IR mergers with OF. (a) IRAS 19254−7245 (through the filter F814W); (b) IRAS 13218+0552 (through F702W); (c) IRAS 23128−5919 (through F814W); (d) IRAS 01003−2238 (through F814W).

southern nucleus, similar to a 'giant SN ring' with $r \sim 4$ kpc and an angle to the line of sight of $i \sim 50^{\circ}$–60° (Lípari et al., in preparation). However, this ring was clearly detected only when the system was located in the PC charge-coupled device (when the southern nucleus was located in the WFC we observed only superimposed and non-detached structures). In addition, our new ESO-NTT high-resolution data – obtained for this ULIR merger – reveal very extended Hα emission in $r \sim 6$–7 kpc around the southern nucleus (including the region of the ring) resembling the extended Hα emission at $r \sim 5$–6 kpc that we found in NGC 3256. Furthermore, the NTT Hα image shows a clear arc around the northern nucleus, on the western side. It is interesting to note that the ring and the arc detected in IRAS 19254−7245 are similar to the double arc/shell observed in Arp 220 (Heckman et al. 1987; $r \sim 5$ kpc); and the presence of two arcs – in Arp 220, and probably in IRAS 19254−7245 – could be explained by the presence of two compact starburst nuclei.

3.5 Wolf–Rayet features in QSOs with strong Fe II emission: PG sample

In this section we present the results of the search for Wolf–Rayet features in the partial PG QSOs sample of Boroson & Green (1992): 87 PG QSOs that have $z \leqslant 0.5$. We note that the original bright Quasar Survey (BQS/PG; Schmidt & Green 1983), is an ultraviolet (UV) excess, magnitude-limited sample ($B_{\rm LIM} = 16.16$) of 114 bright QSOs.

The KPNO spectra (resolution of ∼300 km s^{-1}, covering the rest wavelength range 4300–5700 Å) of these 87 PG QSOs are very interesting since there is a subsample of strong and moderate Fe II emitters (∼25 objects; Boroson & Green 1992). We suggested for some strong Fe II QSOs a composite scenario as the source of nuclear energy (and therefore WR features could be detected). Boroson & Green made available the observed data, and they show – in their fig. 1 – the spectra without the Fe II contribution (i.e. after subtraction of an Fe II template). These facts allowed us to perform a search for WR features in the rest-wavelength range of 4600–4700 Å (the region of the WR emission lines N III λ4640, C IV λ4658 and He II λ4686), for these Fe II QSOs.

In the Fe II PG-QSOs emitters we found four cases with possible WR features: PG 1244+026, 1444+407, 1448+273 and 1535+547 (see Table 4, and Boroson & Green 1992, their fig. 1).

The possible WR features found in PG 1444+407 and 1448+273 are similar to those detected in IRAS 01003−2230 (by Armus et al. 1988); i.e. lines N III λ4640 and He II λ4686 with relatively similar

Table 4. PG QSOs with possible WR features.

PG QSO	z	$\mathrm{FLUX_{WR\lambda4660}}$ erg cm^{-2} s^{-1}	$L_{\mathrm{WR}\lambda4660}$ erg s^{-1}	M_V	Comments
1244+026	0.048	(1.0×10^{-14})	(4.5×10^{40})	−21.77	IRAS F12440+0238
1444+407	0.267	(2.0×10^{-15})	(2.7×10^{41})	−25.18	X-ray source
1448+273	0.065	(5.5×10^{-15})	(4.4×10^{40})	−23.30	X-ray source
1535+547	0.038	(8.2×10^{-15})	(2.3×10^{40})	−22.15	Mrk 486

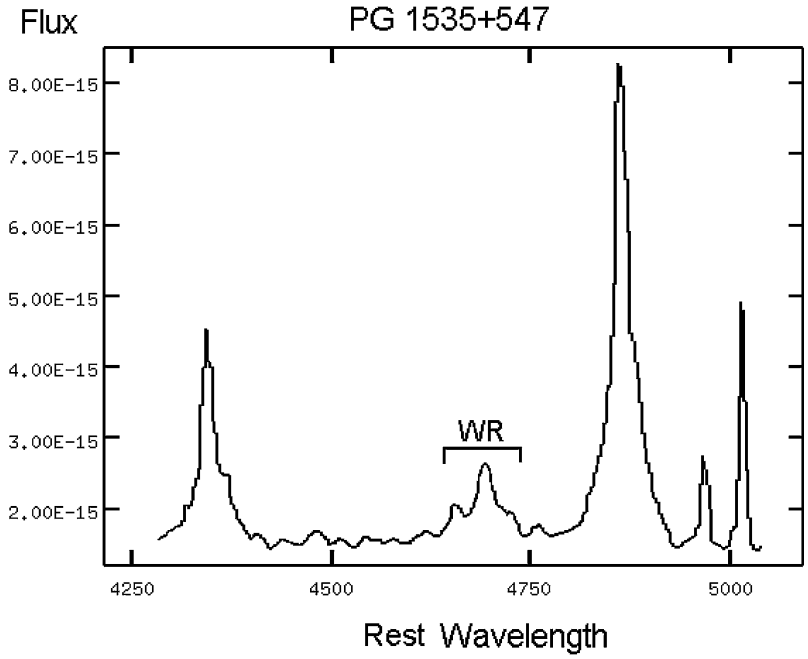

Figure 7. A possible blend of WR features detected in the digitized spectrum of PG QSO 1535+547 (after subtraction of an Fe II template; from Boroson & Green 1992).

weak fluxes. These possible WR features were observed at a S/N ratio in the range ∼3–5. The other two PG QSOs (1244+026 and 1535+547) show possible blends of WR features; and we used the lines N III λ4640 and C IV λ4658 to make the possible identification. However, these two objects show a strong He II λ4686 line; implying a possible contribution from the AGN. We observed these possible blends of WR features at a S/N ratio in the range ∼4–6. Therefore, these four PG QSOs could be considered mainly as candidates for WR features (see Table 4). Fig. 7 shows (as an example) the possible blend of WR features detected in PG 1535+547, after subtraction of an Fe II template. A brief discussion of these results is included in Section 4.2.

Notice the method of subtraction of the Fe II optical template, which is basically the Fe II spectrum of I Zw 1 fitted for each object (Boroson & Green 1992). At the present time it is one of the best available procedures for measuring Fe II and obtaining spectra free of the Fe II contribution (Lawrence et al. 1997). Furthermore, Boroson & Meyers (1992) in their fig. 1 show clearly that the Fe II residuals do not generate 'false' emission lines and do not increase the noise substantially (in the KPNO moderate quality spectra). These two facts give confidence that these PG QSOs are good candidates for having WR features.

4 DISCUSSION

In this section we briefly discuss the main results obtained (a more detailed analysis will be presented with the study of the individual objects). In addition, we review the role of merger, starburst and GW in IR BAL-QSOs and galaxies in formation.

4.1 The galactic-wind and WR features in NGC 4038/39, IRAS 23128−5919 and nearby mergers

Fabbiano et al. (1997), from high-resolution X-ray *ROSAT* images, found extended emission associated with NGC 4039; and they suggested that detailed spectroscopic observations were required in order to study a possible nuclear outflow. The result reported in Section 3.1 shows the first direct kinematic evidence for nuclear outflow in NGC 4039. Which could only be associated with nuclear starburst (and GW), since there is no evidence of AGN properties in all the multiwavelength studies of The Antennae (including new *ISO* observations: Kunze et al. 1996; Fischer et al. 1996; Vigroux et al. 1996). Similar explanations could be given for IRAS 23128−5919: previous studies suggested the presence of outflow and WR features. Our observations at CASLEO, show, at a low S/N ratio, the presence of both features in the bright southern nucleus of this IR merger (Section 4.3).

These and previous results for Arp 220, Mrk 266, 273, NGC 1222, 1614, 3256, 3690, 4194, 6240, and other mergers with both strong starburst and galactic wind (see Heckman et al. 1990), strongly suggest that the relation among merger, starburst, galactic wind and IR emission could play an important role in the evolution and formation of galaxies and AGNs (see Section 4.3).

The mean values of OF – observed in these and previous studies of starburst mergers (Heckman et al. 1990; Lípari et al. 2000; Viegas, Contini & Contini 1999) – lie in the velocity range of $100 \leqslant V_{\rm OF} \leqslant 700$ km s^{-1}. The situation is different for IR mergers with strong starburst+QSOs (see the next section).

4.2 The extreme galactic wind, arcs and WR features in IRAS 01003−2238, 13218+0552 and IR QSOs/galaxies

In Section 3, we found six new objects with EVOF ($V_{\rm OF} > 700$ km s^{-1}). The nearby IR galaxies with EVOF show mainly strong starburst plus the presence of an obscured AGN (see Table 3). This fact suggests that the coexistence of the two main processes of nuclear activity could generate extreme outflow. This result is in agreement with a composite model as the source of nuclear energy in ULIRGs and LIRGs (i.e. starburst plus standard AGN; Perry & Dyson 1992; Dyson, Perry & Williams 1992; Perry 1992; Lípari & Macchetto 1992). It is important to note that previously we found two nearby EVOF objects (Mrk 231 and IRAS 19254−7245) and we associated the presence of outflows and circumnuclear blue arcs with a GW+QSO composite scenario (Lípari et al. 1994; Colina et al. 1991a and Section 3.4).

A very interesting EVOF case was reported by Heckman et al. (1990). They found OF of 1600–2000 km s^{-1} inside of the eastern nuclear bubble in NGC 3079. These authors suggested that the observed very high velocity at kiloparsec scales could only arise in a violent outflow; and they proposed for the origin of the OF a starburst scenario. Filippenko & Sargent (1992) using long-slit spectra confirm this OF detection and proposed an AGN or composite model in order to explain the high values of OF. Veilleux et al. (1994), from a detailed Fabry–Perot interferometric study of the nuclear bubble of NGC 3079 concluded that the central starburst seems to have enough power to supply the bubble OF, and it is possible that an obscured AGN contributes to this OF. Therefore, even for the nearest case of EVOF, it is difficult to discriminate between the possible origin of EVOF (starburst, AGN or composite). However, it is worth noting that NGC 3079 shows EVOF in a nuclear bubble, and the source of nuclear energy is starburst+AGN (Heckman et al. 1990; Filippenko & Sargent 1992). We found a similar composite source of nuclear energy in practically all the nearby EVOF cases (Table 3).

Furthermore, we detected several galactic shell/arcs and rings, in nearby EVOF IR mergers and QSOs (see Section 3); which are probably associated with the starburst+AGN process. It should be studied if these giant galactic shocks – associated with the compression of the ISM by the galactic wind/EVOF – could generate new star formation episodes. This mechanism could produce the 'dense shell of star-forming knots' detected in the arc of Mrk 231; and also the chain/arc of 'extremely blue star-forming knots' in IRAS 01003−2238.

The presence of 'giant arcs, shells or rings' has already been used in order to explain the BAL system in the IR QSO IRAS 07598+6508 (Lípari 1994). Heiles (1992) and Tenorio-Tagle & Bodenheimer (1988) give further references of observational and theoretical studies of giant shells, bubbles and rings, associated mainly with multiple explosions of type II SNe.

In addition, the presence of Wolf–Rayet features in EVOF IR QSOs and probably in several Fe II PG QSOs could be indicative of a large number of massive stars in these objects (see Armus et al. 1988; Conti 1991). This possibility is consistent with a 'composite' model for the source of nuclear energy in some IR QSOs. In Table 4, we present the fluxes and luminosities of the possible WR lines, measured in the four PG QSOs candidates for WR features. This table shows high luminosity values (between 2.3×10^{40} and 2.7×10^{41} erg s^{-1}), when compared with the range found for WR galaxies (see Armus et al. 1988, their table 3; Conti 1991; Schaerer, Contini & Pindao 1999): 9.0×10^{37} (for Mrk 724) and 2.9×10^{41} erg s^{-1} (for IRAS 01003−2238). It is interesting to note that the highest value of WR emission-line luminosity known was detected in an EVOF IR QSO.

Finally, several theoretical works remark on the important role of the starburst and outflow even for the standard AGN model (Collin & Zahn 1999; Collin & Joly 2000) and new models of outflow/wind in AGN were proposed (mainly associated with the accretion discs and jets; see Murray et al. 1995). A detailed discussion of theoretical AGN or composite outflow models is beyond the goals of the present paper. However, we note that the evolutionary end product of the relationship between mergers and extreme starburst/GW could be: (i) supermassive black hole and IR-QSOs in the nuclear region (Rees 1977; Weedman 1983; Sanders et al. 1988a; Norman & Scoville 1988; Taniguchi, Ikeuchi & Shioya 1999b), according to the conditions of the merger+starburst processes, such as the nuclear compression of the ISM gas, the inflow and outflow rate, etc. (Genzel et al. 1998; Downes & Solomon 1998; Taniguchi et al. 1999b; Lípari 1994; Lípari et al. 2000); or (ii) elliptical, cD, radio galaxies for the multiple-merger process as a whole (Toomre 1977; White 1979; Schweizer 1980, 1982; Joseph & Wright 1985; Barnes 1989; Barnes & Hernquist 1992; Kormendy & Sanders 1992; Whitmore et al. 1993, 1999; Sanders & Mirabel 1996; Weil & Hernquist 1996; Shier & Fischer 1998; Genzel et al. 2001).

4.3 The role of merger+starburst+GW in IR BAL QSOs and galaxies in formation

In general, the main role attributed to the galactic-wind component in luminous IR mergers is to clear the ISM from the nuclear regions and probably to unveil a new AGN (see Sanders & Mirabel 1996). In this section we review in the light of our results and new published studies, other roles for the 'extreme' starburst+galactic-wind component; in particular for: (i) IR BAL-QSOs and (ii) galaxies in formation (already suggested by Ostriker & Cowie 1981; Heckman et al. 1990; Berman & Suchkov 1991; Perry 1992; Lípari 1994; Scoville & Norman 1996 and others).

It is important to remark that very recently, detailed new-technology interferometric (IRAM and VLT) and spectroscopic (*ISO*) studies yielding high-resolution data, confirmed the presence of 'extreme' starbursts in ULIRGs: 1000 times as many OB stars as 30 Dor in the IR mergers Mrk 231, Arp 220, 193, Mrk 273 (see Downes & Solomon 1998; Smith et al. 1998; Genzel et al. 1998). In addition, Lípari et al. (2000) using new-technology data (*HST* and ESO NTT) showed that NGC 3256 is another example of a nearby IR merger showing an extended massive star formation process, with a powerful associated galactic wind. Therefore, it is important to study in detail the possible roles of merger, starburst and GW in the evolution of galaxies (where the phases of IR BAL-QSOs and galaxy collision are probably critical steps).

First, the role of the merger+starburst+outflow in IR QSOs must be considered, in particular in BAL IR QSOs; since: (i) Low et al. (1989) and Boroson & Meyers (1992) found that IR-selected QSOs show a 27 per cent low-ionization BAL QSO fraction compared with 1.4 per cent for the optically selected high-redshift QSOs sample (Weymann et al. 1991); (ii) extreme IR galaxies (ULIRGs) are mainly mergers (Section 1); (iii) these objects are also extreme/strong IR+Fe II emitters (Boroson & Meyers 1992; Lípari 1994). Lípari et al. (1993, 1994), Scoville

& Norman (1996), Egami et al. (1996), Lawrence et al. (1997), Terlevich et al. (in preparation) and others proposed that the extreme IR+BAL+Fe II phenomena are related – at least in part – to the end phase of an 'extreme starburst' and the associated 'powerful galactic wind'. At the final stage of a strong starburst, i.e. type II SN phase (8–60 $\times$ 10^6 yr from the initial burst; Terlevich et al. 1992; Norman & Ikeuchi 1989; Suchkov et al. 1994) giant galactic arcs and extreme Fe II+BAL systems can appear. In addition, the early starburst phase dominated by H II regions is associated with large amounts of dust and IR emission (Terlevich et al. 1993; Franco 2002, private communication). This is caused by the dust present in any star formation region and also by the large amount of dust synthesized by the most massive stars during the η-Carinae phase before becoming a WR star (during this phase up to 1 $M_\odot$ of dust per evolved massive star may be injected into the ISM; Terlevich et al. 1993).

Specifically, in the starburst and composite scenarios, two main theoretical models for the origin of BAL systems were proposed: (i) for IR dusty QSOs/galaxies, in the outflowing gas + dust material the presence of discrete trails of debris (shed by individual mass-loss stars) produces the BAL features (Scoville & Norman 1996); and (ii) in SN ejecta, which are shock heated when a fast forward shock moves out into the ISM (with a velocity roughly equal to the ejecta) and a reverse shock accelerates back and moves towards the explosion centre; the suppression of redshifted absorption lines arise since SN debris moving toward the central source are slowed down much more rapidly (by the wind) than is material moving away (Perry & Dyson 1992; Perry 1992). These two alternatives are probably complementary and both explain the main observed properties of the BAL phenomena (Perry 1992; Scoville 1992; Scoville & Norman 1996). Indeed, in the blue arc and the nuclear starburst regions of the BAL/IR QSO Mrk 231 we detected a range of expanding velocities from -500 to -5000 km s^{-1} (in the absorption and/or emission lines; Lípari et al. 1994), which argues for a possible link between starburst+QSO to BAL phenomena.

Furthermore, the presence of large galactic-scale arcs, shells or rings in IR QSOs could be a third explanation (in the starburst and composite scenarios) for the origin of BAL systems in these objects. In which the physical processes could be similar to those suggested by Perry (1992) and Perry & Dyson (1992), but at larger scales ($r \sim$ 2–20 kpc). In addition, recently Tenorio-Tagle et al. (1999) proposed a scenario based on the hydrodynamics of superbubbles powered by massive starburst that accounts for some BAL detected in star-forming galaxies (Kunth et al. 1998). We note that the range of expanding velocities observed in Mrk 231 is exactly that required in order to explain observed BAL systems; and also is consistent with theoretical starburst scenarios where giant expanding arcs or rings generate fast giant shocks in the ISM (Suchkov et al. 1994; Lípari et al. 1994; Tenorio-Tagle, Rozyczka & Bodenheimer 1990). In this third/arc model, the high fraction of IR-selected QSOs showing properties of low-ionization BAL QSOs could be explained by the high fraction of arcs, shells and giant SN rings present in these systems (probably originated in the starburst type II SN phase). In addition, the effects of the orientation of the line of sight and dust obscuration also play important roles (Perry 1992).

Over the last few years Thompson, Hill & Elston (1999) and Elston, Thompson & Hill (1994) reported more than 15 QSOs at redshift $2 < z < 5$, observed at the rest wavelength of UV and optical Fe II + BAL spectral regions. Approximately 50 per cent of these objects show 'strong' Fe II emission, and many of these objects are also BAL+IR QSOs. Thompson et al. (1999) also found a lack of iron abundance evolution in high-redshift QSOs: i.e. the absence of increase in the Fe II/Mg II line ratio and Fe II equivalent width from the earliest epoch ($z = 4.47$ and 3.35) to the present. This represents a problem, since this fact would indicate that 1 Gyr may be an underestimate of the age of the Universe at $z = 4.47$; assuming that type Ia SNe are the dominant source of Fe enrichment in standard models of QSOs. Consequently, q_0 could be $\leqslant 0.20$ for $H_0 =$ 75 km s^{-1} Mpc^{-1}. We emphasize that in our proposed starburst+AGN composite scenario, both results, the detection of strong Fe II in QSOs at redshifts $2 \leqslant z \leqslant 5$ (or even at $z \geqslant 5$), and the lack of iron abundance evolution in high-redshift QSOs, agree with the prediction of our models (Lípari et al. 1993, 1994; Terlevich et al. 1992 , in preparation). Specifically, since in our model the time for the strong Fe enrichment in the shell of type II SNe and in the ISM is $\sim$8–60 $\times$ 10^6 yr (i.e. the end phase of an 'extreme starburst') and this time-scale is very short in relation to that required for the Fe enrichment of the ISM by type Ia SN: i.e. 2 $\times$ 10^9 yr (see Friaca & Terlevich 1998). Therefore, in this scenario, the results obtained by Thompson et al. (1999) do not represent a problem with the present accepted age of the Universe at $z \sim 5$: $\sim 10^9$ yr for $q_0 = 0.5$ and $H_0 = 75$ km s^{-1} Mpc^{-1}.

The results reported are also relevant in the study of high-redshift objects and galaxies in formation, since it is expected that the properties of the initial collapse, merger and starburst+galactic wind play an important role in practically all the scenarios of galaxy formation (see Larson 1974; Ostriker & Cowie 1981; Ikeuchi 1981; Dekel & Silk 1986; Ikeuchi & Ostriker 1986; Lacey & Silk 1991; Berman & Suchkov 1991; Cole et al. 1994). Furthermore, the starburst+galactic wind plays a central role in some particular galaxy formation scenarios, for example in the 'explosive' and 'hot' models (postulated by Ostriker & Cowie 1981 and Berman & Suchkov 1991, respectively) where the SN explosions and galactic wind are the process of star formation self-regulation in young galaxies (see also McKee & Ostriker 1977; Heckman et al. 1990; Lípari et al. 1994). These properties are very similar to those found in Mrk 231 and 'The Super-Antennae' (see Section 3, Lípari et al. 1994), in the observed extended massive star formation and the 'extreme' galactic-wind processes (with their associated shells/arcs).

When we observe locally the GW in luminous IR mergers (Mrk 231, The Super-Antennae, NGC 3256, Arp 220 and others), we are probably observing the feedback processes from massive star formation that may have an important influence in determining the overall structure of galaxies in the general dissipative collapse (Rees & Ostriker 1977; Silk 1977; Kormendy & Sanders 1992; Bekki & Shioya 1998; Martin 1999). In particular, in the early stage of galaxy formation (when the star formation rate is expected to be higher) the galactic wind plays a decisive role in the feedback process: reheating the ISM, and contributing to stopping the initial collapse. Therefore, it would determine the overall structure of galaxies.

SNe of type II are highly concentrated in space and time, and arise from massive stars ($m \geqslant 5\,M_\odot$) in young stellar clusters and associations (of tens or hundreds massive stars; Heiles 1987). The presence of 'extreme' starburst and arcs/shells in ULIRGs (Downes & Solomon 1998; Genzel et al. 1998; Smith et al. 1998; Lípari et al. 1994; Heckman et al. 1990) is also a confirmation of the existence of multiple type II SN explosions. These multiple type II SN explosions are the main galactic process capable of generating the blow-out phase of the galactic winds (arcs and shells), Fe overabundance and the BAL phenomena (Norman & Ikeuchi 1989; Perry & Dyson 1992; Lípari et al. 1993, 1994; Lípari 1994; Taniguchi et al. 1994; Scoville & Norman 1996). However, in the dusty nuclear regions of LIRGs and ULIRGs (with $A_V \sim$ 10–1000 mag; see Sakamoto et al. 1999; Genzel et al. 1998), the presence of type II

super/hypernovae could be detected only for nearby systems and using radio interferometric data (see Smith et al. 1998).

Finally, new submillimetre-wavelength surveys show a population of very dusty star-forming galaxies at high redshift (Smail, Ivison & Blain 1997; Hughes et al. 1998; Berger et al. 1998), with very similar properties to those observed in ULIRGs mergers (Scott 1998). Therefore, in order to study 'extreme/primordial starbursts' in distant IR mergers and very dusty IR galaxies, clear signals are the above described features, associated with the presence of powerful galactic winds, 'multiple' type II SN explosions and starburst+AGN (e.g. galactic-shells/arcs, spectra with outflow or WR components, very blue spiral arms, etc.). These features are similar to those observed – at low redshift – in Mrk 231, Arp 220, NGC 3256, IRAS 19254−7245, 01003−2238, 07598+6508, 13218+0552, 04505−2958 and others.

5 SUMMARY AND CONCLUSIONS

In this paper we have presented mainly optical spectroscopy (obtained at ESO, KPNO, MKO, CASLEO and BALEGRE) and deep *HST* WFPC2 broad-band images of selected IR mergers and IR QSOs. The main results and conclusions can be summarized as follows.

(i) We found and discussed detailed kinematic and/or morphological evidence for OF and WR features, in the nearby IR mergers NGC 4038/39, IRAS 23128−5919 (with low-velocity OF) and in the nearby QSOs IRAS 01003−2238 and 13218+0552 (with extreme velocity OF).

(ii) We found kinematic evidence for EVOF (from a study of a complete sample of ULIRG and QSOs, 'The IRAS 1-Jy MKO-KPNO Survey') in IRAS 11119+3257, 14394+5332, 15130–1958 and 15462−0450. From this sample, we also detected probably OF in IRAS 05024−1941, 13305−1739, 13451+1232 and 23389+0300.

(iii) We found that the low-velocity OF components were detected mainly in objects with starburst processes, i.e. OF associated with galactic winds generated in multiple type II SN explosions and massive stars. Meanwhile the EVOF were detected mainly in objects with strong starburst plus obscured IR QSOs; which suggests that the coexistence of both processes could generate EVOF.

(iv) *HST* archive images of IR+BAL+Fe II QSOs show in practically all of these objects 'arc or shell' features probably associated with galactic winds (i.e. to multiple type II SN explosions or to starburst+AGN) and/or merger processes.

(v) We analyse the presence of Wolf–Rayet features in part of the large sample of bright PG-QSOs, and nearby galaxies with galactic wind. We found possible WR features in the Fe II PG-QSOs: PG 1244+026, 1444+407, 1448+273 and 1535+547.

Finally, we briefly discuss these results mainly within the framework of the composite (starburst+AGN) scenario. We also comment on the role of mergers, starburst and galactic wind in our proposed scenario of young/composite IR QSOs (which probably evolved from IR mergers).

ACKNOWLEDGMENTS

This paper is based on observations obtained at European Southern Observatory (Chile), *Hubble Space Telescope* satellite (NASA/ESA), Bosque Alegre Astrophysical Station (Argentina), Complejo Astronómico El Leoncito (Argentina), Kitt Peak National Observatory (USA), Mauna Kea Observatory, Hawaii (USA). The authors thank P. Amram, J. Boulesteix, G. Goldes, L. Hernquist and J. Hibbard for discussions and help. We wish to thank T. Boroson, R. Green, D. Kim, D. Sanders and S. Veilleux for the MKO and KPNO spectra (The IRAS 1-Jy Survey of ULIRG and PG QSO Sample), kindly made available to us. We would like to express our gratitude to the staff members and observing assistants at BALEGRE, CASLEO and ESO Observatories. This work was based on observations made using the NASA and ESA *HST* satellite, obtained from archive data at ESO-Garching and STScI-Baltimore. This paper was made using the NASA Extragalactic Data base NED; which is operated by the Jet Propulsion Laboratory, California Inst. of Technology, under contract with NASA. This research was supported in part by Grants from Conicet, SeCyT-UNC and Fundación Antorchas (Argentina). Finally, we wish to thank the referee for constructive and valuable comments, which helped to improve the content and presentation of the paper.

REFERENCES

Afanasiev V., Dodonov S., Carranza G., 1994, Bol. Asoc. Argentina Astron., 39, 160
Armus L., Heckman T.M., Miley G., 1988, ApJ, 326, L45
Armus L., Surace J., Soifer B., Matthews K., Graham J., Larkin J., 1994, AJ, 108, 76
Barnes J., 1989, Nat, 338, 123
Barnes J., Hernquist L., 1992, ARA&A, 30, 705
Beichman C.A., Soifer B., Helou G., Chester T., Neugebauer G., Gillett F., Low F., 1986, ApJ, 308, L1
Bekki K., Shioya Y., 1998, ApJ, 497, 108
Berger A.J., Cowie L., Sanders D., Fulton E., Taniguchi Y., Sato Y., Kawara K., Okuda H., 1998, Nat, 394, 248
Bergvall N., Johansson L., 1985, A&A, 149, 475
Berman B., Suchkov A., 1991, Ap&SS, 184, 169
Bevington P., 1969, Data Reduction and Error Analysis for the Physical Sciences. McGraw-Hill, New York
Boroson T., Green R., 1992, ApJS, 80, 109
Boroson T., Meyers K., 1992, ApJ, 397, 442
Boyce P.J. et al., 1996, ApJ, 473, 760
Canalizo G., Stockton A., 1997, ApJ, 480, L5
Canalizo G., Stockton A., Roth K., 1998, AJ, 115, 890
Clements D., Sutherland W., Saunders W., Efstathiou G., McMahon R., Maddox S., Lawrence A., Rowan-Robinson M., 1996, MNRAS, 279, 459
Cole S., Aragon-Salamanca A., Frenk C., Navarro J., Zepf S., 1994, MNRAS, 271, 781
Colina L., Lípari S.L., Macchetto F., 1991a, ApJ, 379, 113
Colina L., Lípari S.L., Macchetto F., 1991b, ApJ, 382, L63
Collin S., Joly M., 2000, New Astron. Rev., 44, 531
Collin S., Zahn J., 1999, A&A, 344, 433
Conti P.S., 1991, ApJ, 377, 115
Conti P.S., Vacca W.D., 1994, ApJ, 423, L97
Dekel A., Silk J., 1986, ApJ, 303, 39
Díaz R., Carranza G., Dottori H., Goldes G., 1999, ApJ, 512, 623
Downes D., Solomon P.M., 1998, ApJ, 507, 615
Dyson J., Perry J., Williams R., 1992, in Holt S., Neff S., Urry M., eds, Testing the AGN Paradigm. AIP, New York, p. 548
Egami E., Iwamuro F., Maihara T., Oya S., Cowie L., 1996, AJ, 112, 73
Elston R., Thompson K., Hill J., 1994, Nat, 367, 250
Fabbiano G., Schweizer F., Mackie G., 1997, ApJ, 478, 542
Filippenko A., Sargent W., 1992, AJ, 103, 28
Friaca A., Terlevich R., 1998, MNRAS, 298, 399
Fischer J. et al., 1996, A&A, 315, L97
Genzel R. et al., 1998, ApJ, 498, 579
Genzel R., Tacconi L., Rigopoulou D., Lutz D., Tecza M., 2001, ApJ, 563, 527
Heckman T.M., Armus L., Miley G., 1987, AJ, 93, 276

Heckman T.M., Armus L., Miley G., 1990, ApJS, 74, 833
Heiles C., 1987, ApJ, 315, 555
Heiles C., 1992, in Palous J., Burton W., Lindblad P., eds, Proc. Evolution of ISM and Dynamics of Galaxies. Cambridge Univ. Press, Cambridge, p. 12
Hines D., Wills B., 1995, ApJ, 448, L69
Hines D., Low F., Thompson R., Weymann R., Storri-Lanbardi L., 1999, ApJ, 512, 140
Hughes D.H. et al., 1998, Nat, 394, 241
Ikeuchi S., 1981, PASJ, 33, 211
Ikeuchi S., Ostriker J., 1986, ApJ, 301, 522
Johansson L., Bergvall N., 1988, A&A, 192, 81
Joseph R.D., Wright G., 1985, MNRAS, 214, 87
Kim D., Sanders D., 1998, ApJS, 119, 41
Kim D., Veilleux S., Sanders D., 1998, ApJ, 508, 627
Kormendy J., Sanders D., 1992, ApJ, 390, L53
Kunth D., Mas-Hesse J., Terlevich E., Terlevich R., Lequeux J., Fall S., 1998, A&A, 334, 11
Kunze D. et al., 1996, A&A, 315, L101
Lacey C., Silk J., 1991, ApJ, 381, 14
Larson R., 1974, MNRAS, 169, 229
Lawrence A., Sanders W., Rowan-Robinson M., Crawford J., Ellis R., Frenk C., Efstathiou G., Kaiser N., 1988, MNRAS, 235, 261
Lawrence A., Elvis M., Wilkes B., McHardy I., Brandt N., 1997, MNRAS, 285, 879
Lípari S.L., 1994, ApJ, 436, 102
Lípari S.L., Macchetto F., 1992, ApJ, 387, 522
Lípari S.L., Macchetto F., Golombeck D., 1991, ApJ, 366, L65
Lípari S.L., Terlevich R., Macchetto F., 1993, ApJ, 406, 451
Lípari S.L., Colina L., Macchetto F., 1994, ApJ, 427, 174
Lípari S.L., Tsvetanov Z., Macchetto F., 1997, ApJS, 111, 369
Lípari S.L., Diaz R., Taniguchi Y., Terlevich R., Dottori H., Carranza G., 2000, AJ, 120, 645
Lípari S.L., Mediavilla E., Diaz R., 2001, in Claria J., Levato H., Peimbert S., eds, X Reunion Latino Americana de Astronomia. Rev. Mexicana Astron. Astrof., in press
Low F., Cutri R., Huchra J., Kleinmann S., 1988, ApJ, 327, L41
Low F., Cutri R., Kleinmann S., Huchra J., 1989, ApJ, 340, L1
Lutz D., Veilleux S., Genzel R., 1999, ApJ, 517, L13
Martin C., 1999, ApJ, 513, 156
McKee C., Ostriker J., 1977, ApJ, 218, 148
Melnick J., Mirabel I.F., 1990, A&A, 231, L19
Mihos C., Hernquist L., 1994a, ApJ, 425, L13
Mihos C., Hernquist L., 1994b, ApJ, 431, L9
Mihos C., Hernquist L., 1996, ApJ, 464, 641
Murray N., Chiang J., Grossman S., Voit G., 1995, ApJ, 451, 498
Norman C., Ikeuchi S., 1989, ApJ, 395, 372
Norman C., Scoville N., 1988, ApJ, 332, 124
Ostriker J., Cowie L., 1981, ApJ, 243, L127
Perry J., 1992, in Filippenko A., ed., ASP Conf. Ser. Vol. 31, Relationships Between AGN and Starburst Galaxies. Astron. Soc. Pac., San Francisco, p. 169
Perry J., Dyson R., 1992, in Holt S., Neff S., Urry M., eds, Testing the AGN Paradigm. AIP, New York, p. 553
Read A., Ponman T., Wolstencroft R., 1995, MNRAS, 277, 397
Rees M., 1977, ARA&A, 42, 471
Rees M., Ostriker J., 1977, MNRAS, 179, 541
Remillard R., Bradt H., Brissenden R., Buckley D., Robert D., Schwartz D., Stroozas B., Tuohy I., 1993, AJ, 105, 2079
Rieke G., Cutri R., Black J., Kailey W., McAlary C., Lebofsky M., Elston R., 1985, ApJ, 290, 116
Rosa M., D'Oddorico S., 1986, in de Loore C., Willis A., Laskarides P., eds, Proc. IAU Symp. 116. Reidel, Dordrecht, p. 355
Sakamoto K., Scoville N., Yun M., Crosas M., Genzel R., Tacconi L., 1999, ApJ, 514, 68
Sanders D.B., Mirabel F., 1996, ARA&A, 34, 749
Sanders D.B., Soifer B.T., Elias J.H., Madore B.F., Matthews K., Neugebauer G., Scoville N.Z., 1988a, ApJ, 325, 74
Sanders D.B., Soifer B.T., Elias J.H., Neugebauer G., Matthews K., 1988b, ApJ, 328, L35
Schaerer D., Contini T., Pindao M., 1999, A&AS, 136, 35
Schinnerer A., Eckart A., Tacconi L., 1998, ApJ, 500, 147
Schmidt M., Green R., 1983, ApJ, 269, 352
Schweizer F., 1980, ApJ, 237, 303
Schweizer F., 1982, ApJ, 252, 455
Schweizer F., 1996, AJ, 111, 109
Scott D., 1998, Nat, 394, 219
Scoville N.Z., 1992, in Filippenko A., ed., ASP Conf. Ser. Vol. 31, Relationships Between AGN and Starburst Galaxies. Astron. Soc. Pac., San Francisco, p. 159
Scoville N.Z., Norman C., 1996, ApJ, 451, 510
Scoville N.Z., Soifer B.T., 1991, in Leitherer C., Walborn N., Heckman T.M., Norman C., eds, Massive Stars in Starbursts. Cambridge Univ. Press, Cambridge, p. 233
Silk J., 1977, ApJ, 211, 638
Shier L., Fischer J., 1998, ApJ, 497, 163
Smail I., Ivison R., Blain A., 1997, ApJ, 490, L5
Smith H., Lonsdale C., Lonsdale C., Diamond P., 1998, ApJ, 493, L17
Stockton A., Canalizo G., Close L., 1998, ApJ, 500, L121
Stone R., Baldwin J., 1983, MNRAS, 204, 357
Suchkov A., Balsara D., Heckman T., Leitherer C., 1994, ApJ, 430, 511
Surace J., Sanders D., Vacca W., Veilleux S., Mazzarela J., 1998, ApJ, 492, 116
Taniguchi Y., Kawara K., Murayama T., Sato Y., 1994, AJ, 107, 1668
Taniguchi Y., Yoshino A., Ohyama Y., Nishiura S., 1999a, ApJ, 514, 660
Taniguchi Y., Ikeuchi S., Shioya K., 1999b, ApJ, 514, L9
Tenorio-Tagle G., Bodenheimer P., 1988, ARA&A, 26, 145
Tenorio-Tagle G., Rozyczka M., Bodenheimer P., 1990, A&A, 237, 207
Tenorio-Tagle G., Silich S., Kunth D., Terlevich E., Terlevich R., 1999, MNRAS, 309, 332
Terlevich R., Tenorio-Tagle G., Franco J., Melnick J., 1992, MNRAS, 255, 713
Terlevich R. et al., 1993, in Rocca-Volmerange B., Dennefeld M., Guiderdoni B., Tran Thanh Van, eds, First Light in the Universe, Star or QSOs. Editions Frontieres, Paris, p. 261
Thompson K., Hill J., Elston R., 1999, ApJ, 515, 487
Tomisaka K., Ikeuchi S., 1988, ApJ, 330, 695
Toomre A., 1977, in Tinsley B., Larson R., eds, The Evolution of Galaxies and Stellar Population. Yale Univ. Observatory, New Haven, p. 401
Vader J.P., Da Costa G., Heeisler Ch., Frogel J., Simon M., 1987, AJ, 94, 847
Veilleux S., Bland-Hawthorn J., Tully R., Filippenko A., Sargent W., 1994, ApJ, 433, 48
Veilleux S., Kim D., Sanders D., 1999, ApJ, 522, 113
Viegas S., 1999, A&A, 347, 112
Vigroux L. et al., 1996, A&A, 315, L93
Weil M., Hernquist L., 1996, ApJ, 460, 101
Weedman D., 1983, ApJ, 266, 479
Weymann R., Morris S., Foltz C., Hewit P., 1991, ApJ, 373, 23
White S., 1979, MNRAS, 189, 831
Whitmore B., Schweizer F., Leitherer C., Borne K., Robert C., 1993, AJ, 106, 1354
Whitmore B., Zhang Q., Leitherer C., Fall S., Schweizer F., Miller B., 1999, AJ, 118, 1551
Wills B., Wills D., Evans N., Natta A., Thompson K., Breger M., Sitko M., 1992, ApJ, 400, 96

This paper has been typeset from a TEX/LATEX file prepared by the author.